THE AMERICAN SOCIETY OF MECHANICAL ENGINEERS
345 E. 47th St., New York, N.Y. 10017

97-GT-469

THE INFLUENCE OF WAKE-WAKE INTERACTIONS ON LOSS FLUCTUATIONS OF A DOWNSTREAM AXIAL COMPRESSOR BLADE ROW

G. J. Walker

J D Hughes
Department of Civil & Mechanical Engineering
University of Tasmania
Hobart, Australia

I Köhler
Fachgebiet Gasturbinen und Flugantriebe
Technische Hochschule Darmstadt
Germany

W J Solomon
Department of Civil & Mechanical Engineering
University of Tasmania
Hobart, Australia

ABSTRACT

The interaction between wakes of an adjacent rotor-stator or stator-rotor blade row pair in an axial turbomachine is known to produce regular spatial variations in both the time-mean and unsteady flow fields in a frame relative to the upstream member of the pair. This paper examines the influence of such changes in the free-stream disturbance field on the viscous losses of a following blade row. Hot-wire measurements are carried out downstream of the outlet stator in a 1.5-stage axial compressor having equal blade numbers in the inlet guide vane (IGV) and stator rows. Clocking of the IGV row is used to vary the disturbance field experienced by the stator blades: the influence on stator wake properties is evaluated. The magnitude of periodic fluctuations in ensemble-average stator wake thickness is significantly influenced by IGV wake-rotor wake interaction effects. The changes in time-mean stator losses appear marginal.

NOMENCLATURE

a	Circumferential offset of stator blade leading edge from center of IGV wake avenue
c	Blade chord
i	Blade incidence
s	Blade pitch
$s^* = y/s$	Dimensionless circumferential position
t	Time
$t^* = t/T$	Dimensionless time
u	Streamwise velocity
$\overline{u}_s$	Pitch-wise average velocity
w_1	Relative inlet velocity
y	Circumferential distance
$H = \delta^*/\theta$	Shape factor
$Re_1 = w_1 c/\nu$	Chord Reynolds number
$Re_{ref} = U_{mb} c/\nu$	Reference Reynolds number
T	Rotor blade passing period
Tu	Random disturbance level (turbulence)
Tu_D	Total disturbance level
$\tilde{T}u$	Periodic disturbance level (unsteadiness)
U	Local free stream velocity
U_{inv}	Hypothetical inviscid velocity
U_{mb}	Rotor mid-span velocity
V_a	Mean axial velocity
δ^*	Displacement thickness
α	Flow angle from axial
$\phi = V_a/U_{mb}$	Flow coefficient
θ	Momentum thickness
ν	Kinematic viscosity

Superscripts, etc.

$\langle\ \rangle$	Ensemble (phase-lock) average value
$\bar{}$	Time-mean value
$'$	Instantaneous fluctuation from time-mean
$''$	Instantaneous fluctuation from ensemble mean

INTRODUCTION

It has long been appreciated from studies such as those of Smith Jr. (1966), Kerrebrock and Mikolajczak (1970), Lockhart and Walker (1974) and Zierke and Okiishi (1982) that wake dispersion and mixing effects in an axial turbomachine with multiple blade rows may cause uneven energy addition and redistributions of losses and high temperature fluid, with resultant periodic circumferential variations in both the time-mean and unsteady flow fields. The early investigation by Walker (1974) also showed that the periodic disturbances associated with passing wakes may produce periodic unsteady transition phenomena on the surfaces of axial turbomachine blades. However, the complexity of the problem has largely precluded any significant consideration of these effects in axial turbomachine design.

Presented at the International Gas Turbine & Aeroengine Congress & Exhibition
Orlando, Florida — June 2–June 5, 1997

Improvements in computing power and high-speed data acquisition capability have brought a renewed interest in this field in recent years. Further analytical and numerical studies of the influence of rotor-stator axial gap on axial compressor performance have been reported by Deregel and Tan (1996) and Adamczyk (1996). They examine the potential for performance improvement by passing a wake through a blade row prior to being mixed out by viscous diffusion, and indicate potential increases in efficiency and pressure rise of one or two percent. These analyses do not, however, account for variations in blade losses which may accompany a change in the free-stream disturbance field.

Suryavamshi et al. (1996) reported total temperature and pressure measurements downstream of an embedded stator in a multistage axial compressor which clearly show periodic circumferential variations associated with interactions between upstream rotor and stator wakes. Variations in efficiency of 2.5% between the best and worst rotor blades were observed at the stator mid-pitch location. Similar clocking effects in a multistage turbine were investigated numerically by Eulitz et al. (1996). They predicted an efficiency improvement of 0.4% when the dispersed wake street of an upstream stator was incident on the downstream vane, but the model assumed a fully turbulent flow and ignored unsteady wake-induced transition effects on the downstream vanes.

The recent experiments of Halstead et al. (1995), Solomon and Walker (1995a,b) and Solomon (1996) have indicated that transitional flow may cover as much as 70% of compressor airfoil suction surfaces and 50% of turbine airfoil suction surfaces in the presence of periodic wake disturbances. The periodic transitional or turbulent flow strips generated by wake disturbances are followed by regions of relaxing laminar flow with a shear stress higher than steady laminar flow levels. Independent studies of the latter phenomena in a compressor rotor (Cumpsty et al., 1995), turbine cascade (Schulte and Hodson, 1996) and triggered turbulent spot and compressor experiments (Gostelow et al., 1996) have shown these "calmed" regions to be more stable and resistant to separation than a steady laminar boundary layer flow. More extensive surveys of periodic transition effects and their importance in relation to blading design for axial turbomachines can be found in discussions by Hourmouziadis (1989), Mayle (1991,1992) and Walker (1993).

The present paper investigates the influence on blade losses of free-stream disturbance field variations associated with wake dispersion and interaction effects in a 1.5 stage axial compressor. This is achieved by examining the influence of inlet guide vane (IGV) clocking on the viscous losses of the outlet stator blades. The work is partly motivated by an interest in wake-induced transition phenomena and a resulting desire to identify cases of interest for more detailed unsteady boundary layer measurements on the stator blades. We also wish to know how variations in free-stream unsteadiness produced by changing rotor-stator axial gaps might affect the performance characteristics of an axial turbomachine blade row. Will potential efficiency gains from reduced mixing losses in upstream blade wakes be enhanced or diminished by associated changes in downstream blade row losses as the axial gap is altered? And might such efficiency gains be accompanied by some other penalty such as reduced stall margin? The optimisation of axial gap is outside the scope of this paper. However, the ultimate resolution of this problem requires a proper appreciation of the influence of wake mixing and interaction effects on blade losses.

EXPERIMENTAL DETAIL

Research Compressor

Air enters the compressor radially through a cylindrical screened inlet 2.13 m diameter by 0.61 m wide. A flared bend with a 6.25 to 1 contraction ratio then turns the flow through 90° into a concentric cylindrical duct with 1.14 m outside diameter and 0.69 m inside diameter which contains the compressor blade rows. Downstream of the compressor there is an annular diffuser, and a cylindrical sliding throttle at the outlet is used to control the throughflow.

The compressor is a 1.5-stage axial flow machine with three blade rows: inlet guide vanes (IGV), rotor and stator. Fig. 1 shows a cross-section of the compressor blading at mid-passage. There are 38 blades in each of the stationary rows and 37 blades in the rotor, giving space/chord ratios at mid-blade height of 0.99 and 1.02 respectively. The blades all have a constant chord of 76.2 mm and an aspect ratio of 3.0. The blade sections were designed for free vortex flow with 50% reaction at mid-blade height at a flow coefficient ($\phi = V_a/U_{mb}$) of 0.76. The design values of inlet and outlet blade angles from axial at mid-blade height are, respectively: IGV 0.0°, 27.8°; rotor and stator 45.0°, 14.0°. However, for these tests the rotor was restaggered by 2.0° to give blade angles of 43.0° and 12.0° with a resultant increase in stalling flow coefficient.

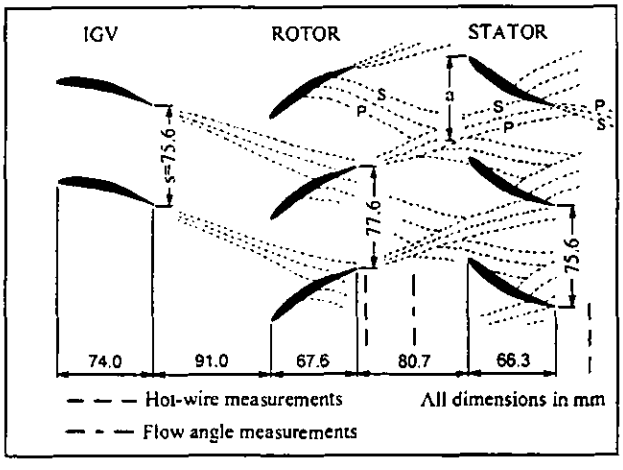

FIGURE 1: Cross-section of compressor blading at mid-passage, showing typical instantaneous wake dispersion. S = suction side; P = pressure side.

Instrument slots in the outer casing of the compressor allow radial and axial traversing of measuring probes at a fixed circumferential position. The IGV and stator rows are each mounted on rotatable supporting rings to permit circumferential traversing of these blades relative to a stationary probe or clocking of one row relative to the other.

Further details of the research compressor can be found in Oliver (1961), Walker (1972) and Solomon (1996).

Range of Investigation

All measurements were conducted at mid-span, where radial flows are small. Data were obtained for flow coefficients ($\phi = V_a/U_{mb}$) of 0.600, 0.675 and 0.840. These correspond, respectively, to incidence values of 4.1°, 1.2°and -6.1°, and will be referred to as high, medium and low loading cases. The medium loading case is close to the Howell (1945) nominal incidence value of 0.6°.

A constant reference Reynolds number of Re_{ref} = 120000 was used for all tests. This gives stator inlet Reynolds numbers of Re_1 = 107000, 112000 and 123000 for the high, medium and low loading cases. These values are low compared with those typical of aircraft gas turbine engine operation, as reported by Hourmouziadis (1989) and Mayle (1991); they are also generally lower than those in the experimental studies of Halstead et al. (1995). The test compressor was nevertheless operating above the critical Reynolds number range where laminar separation starts to cause a significant increase in blade losses (see Walker, 1975). As discussed by Solomon (1996) the critical Reynolds number for the test machine is lower than that for modern compressors because of the generally milder pressure gradients on the suction surface of C4 blading. Surface hot film observations on the stator blading reported by Solomon and Walker (1995a,b) show essentially similar behavior to that in the higher Reynolds number multistage compressor experiments of Halstead et al. (1995).

The influence of IGV clocking on the stator losses was investigated through hot wire measurements acquired at an axial distance of 13.3% chord downstream of the stator for values of a/s = 0.00, 0.25, 0.50 and 0.75. The coordinate a is the circumferential distance of the stator leading edge from the center of the avenue of dispersed IGV wake segments, as shown in Fig. 1. Hot wire observations were also obtained at an axial distance of 5.5% chord dowstream of the rotor to indicate the stator inflow disturbance field. Measurements at this near wake position indicate the IGV wake dispersion process without the complications of subsequent IGV wake-rotor wake interactions. They also give a clearer indication of unsteady rotor blade surface phenomena.

Measurement Techniques

The compressor and measurement systems were controlled by two IBM-compatible 486 personal computers. One computer was used to control the compressor and acquire data from slow response instrumentation. The other was used for high speed data acquisition from the hot wire anemometer. Operating speeds at Re_{ref} = 120000 were typically 500 rpm, and the compressor speed was continuously adjusted with a speed setting accuracy of ± 0.1 rpm to maintain constant Reynolds number. The throttle setting was left unchanged for an individual flow traverse, after setting the desired flow coefficient prior to the start of measurement.

Hot wire measurements were obtained with a TSI IFA-100 system containing TSI Model 150 anemometer bridges and TSI Model 157 signal conditioners. A Dantec 55P03 probe with sensor and support both oriented radially was used for the measurements downstream of the rotor. Measurements behind the stator were obtained with a Dantec 55P01 probe oriented with the sensor parallel to the stator trailing edge. The latter probe was supported from downstream by a mounting tube aligned approximately with the local flow direction. The frequency response of the probes was better than 70 kHz. This is much higher than the rotor blade passing frequency of around 300 Hz in these tests.

The anemometer output was backed with a DC offset voltage and low-pass filtered at 20 kHz before sampling and digitizing at 50 kHz and data storage. The DC offset and signal amplification were adjusted automatically by the data acquisition computer for each spatial measurement point to optimise the signal to noise ratio. Ensemble-average values of measured quantities were obtained from 512 records, with sampling triggered at the same point on each rotor revolution from an optical encoder on the motor end of the drive shaft so that the wakes of the same rotor blades were observed in each record. Each record consisted of 1024 samples, and covered about 6 rotor blade passing periods. Circumferential traverses used 32 points per blade spacing, with a greater concentration of measurement points in wake regions. Time-mean flow data were determined from separate sets of observations with continuous sampling at random phase relative to the rotor motion and an averaging time of about 30 seconds.

The hot wire probes were calibrated in situ in the compressor against velocity data obtained from prior measurements with slow response pressure probes. Calibration drift was monitored during each traverse and corrected by assuming a linear variation in the calibration with time. Velocity values were evaluated digitally for each sample point from the full dimensionless heat transfer relation for the probe, as discussed by Solomon (1996).

Preliminary hot wire measurements downstream of the stator with different relative circumferential settings of the inlet guide vanes were conducted at ϕ = 0.675 to determine the datum position ($a/s = 0$) corresponding to alignment of the stator leading edge with the center of the IGV wake avenue. The circumferential streamline shift with flow coefficient was then computed to estimate the corresponding datum stator positions for the other two loading cases. Subsequent detailed measurements indicate an accuracy of about 0.05 in the values of a/s. Circumferential traverses downstream of the stator were conducted by jointly indexing the IGV and stator rows relative to the fixed probe for each chosen IGV/stator index configuration a/s.

Slow response pressure measurements with a United Sensor CA-120 3-hole cobra probe were used to obtain pitch-averaged flow angle data at 54% chord axial distance upstream of the stator. Local pressure probe measurements over a range of compressor speeds were obtained at convenient stations in the hot wire traverse planes to provide data for in-situ anemometer calibrations. No significant differences were observed between the calibration curves for different axial stations, even though some variable influence of flow unsteadiness on the slow response probe might have been expected.

Disturbance and Turbulence Level Analysis

The reduction of turbulence and unsteadiness data from the hot wire measurements follows the procedure of Evans (1975) with some changes in notation. The instantaneous velocity may be expressed as

$$u = \overline{u} + u' = \langle u \rangle + u'' \qquad (1)$$

where $\overline{u}$ is the long-term time-mean of a continuous record, and $\langle u \rangle(t_i)$ is the ensemble average of N samples at time t_i relative to

the rotor phase reference, defined by

$$\langle u \rangle(t_i) = \frac{1}{N} \sum_{k=1}^{N} \{u(t_i)\}_k \tag{2}$$

The ensemble average velocity only exhibits blade-to-blade periodicity in the test machine, due to the equal blade counts in the IGV and stator rows.

The periodic disturbance level or "unsteadiness" is defined by

$$\tilde{T}u = (\langle u \rangle - \overline{u})_{rms}/U \tag{3}$$

Values of $\tilde{T}u$ must be evaluated from averages over an integral number of blade-passing periods.

The random disturbance level or "turbulence" associated with fluctuations about the ensemble average value is given by

$$Tu = u''_{rms}/U \tag{4}$$

and the total disturbance level associated with fluctuations about the long-term mean is given by

$$Tu_D = u'_{rms}/U \tag{5}$$

Assuming $(\langle u \rangle(t) - \overline{u})$ and u'' to be statistically independent, the three disturbance levels are related by

$$Tu_D^2 = \tilde{T}u^2 + Tu^2 \tag{6}$$

OBSERVATIONS AND DISCUSSION

IGV Wake Dispersion by Rotor

The variation of IGV wake dispersion with flow coefficient, obtained from a circumferential hot wire traverse immediately downstream of the rotor, is shown in Fig. 2. These data were acquired by moving the IGV and stator rows together at a fixed circumferential offset ($a/s = 0.0$). This was done as a precaution even though previous measurements for the medium loading case had shown no measurable influence of the stator circumferential position on the unsteady flow field at this station. The data were obtained over one IGV pitch only, but have been plotted over two blade pitches by assuming pitch-wise periodicity. Ensemble average velocity (non-dimensionalized by pitch-wise average time-mean velocity) is indicated by shading. The line contours indicate ensemble average values of random velocity fluctuations about the ensemble mean (or "turbulence").

This figure represents the instantaneous spatial distribution which would be observed on a cylindrical surface if the flow disturbances were convected unaltered downstream of the measuring station with zero whirl. The variable s^* on the axis represents dimensionless circumferential position relative to the inlet guide vanes. Dimensionless time t^* on the abscissa has been plotted in the reverse direction so that the earliest observed points appear at the right, corresponding to the furthest downstream axial position. The data have been time-shifted to make the rotor-IGV relative circumferential position constant for each probe relative position s^*. This is necessary because the IGV was clocked relative to the trigger point which was fixed relative to the machine and the probe.

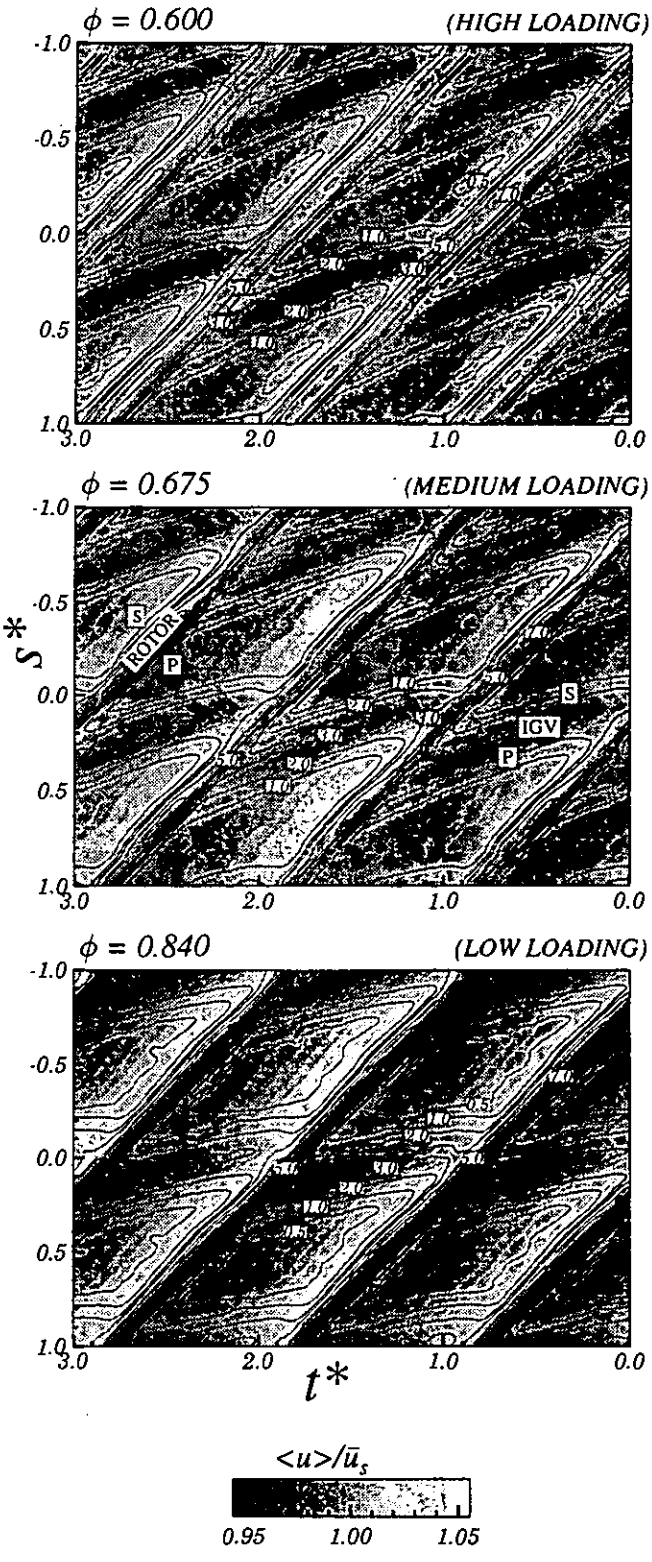

FIGURE 2: Variation of IGV wake dispersion with flow coefficient. Hot-wire measurements 5.5% chord axially downstream of rotor trailing edge at mid-passage. Line contours indicate ensemble average turbulence level, $\langle Tu \rangle$ (%). Re_{ref} = 120,000. S = suction side; P = pressure side.

The rotor wakes can be identified as the parallel bands of high turbulence running diagonally from bottom left to top right as in Fig. 1. The avenue of dispersed IGV wake segments runs horizontally from left to right. This differs from the picture in Fig. 1 because whirl velocity has been ignored. The suction and pressure surface sides of both IGV and rotor wakes (indicated by symbols S and P) are at the top and bottom of the wake regions, respectively.

The rotation of the IGV wake segments relative to the local flow direction increases with rotor blade loading as the flow coefficient is decreased from 0.840 to 0.600. The curvature of the IGV wake segments near the suction side of the rotor wake indicates a retardation of flow by the rotor suction surface boundary layer, which can be seen to thicken as loading is increased. This feature is very similar to the numerical predictions of Deregel and Tan (1996). The peak turbulence level in the IGV wakes is about 3%, whilst the minimum turbulence level in the free-stream (corresponding to inflow regions uncontaminated by wakes) is about 0.5%.

The rotor wakes exhibit periodic variations in thickness indicative of blade loss fluctuations, and gradually thicken as loading is increased (as indicated by separation of the 1% turbulence contours). There is a strong gradient in ensemble average velocity across the rotor blade passage at $\phi = 0.840$. This decreases as loading is increased, and is evidently a potential flow effect. A common feature observed at all loadings is a region of higher velocity in the corner between the suction side of the rotor wake and the pressure side of the IGV wake segment. This may be partly due to the negative jet effect of the relative flow in the IGV wake. The higher rotor wake turbulence level at low loading (which may appear anomalous) is thought to result from the proximity of the suction surface transition zone to the rotor blade trailing edge.

Stator Outlet Flow Field

Similar plots of the flow field downstream of the stator are presented in Fig. 4 for the medium loading case, $\phi = 0.675$. The stator wakes appear as horizontal bands of high turbulence. The suction and pressure sides of the various wake segments are again denoted by S and P. These figures have been complemented by the distributions of dimensionless time-mean velocity $\overline{u}/\overline{u}_s$ and total disturbance level Tu_D plotted at left. $\overline{u}_s$ is the pitchwise average time-mean velocity.

Separate figures are shown for values of $a/s = 0.00$, 0.25, 0.50 and 0.75 to indicate the effect of clocking the stator relative to the IGV wake street. The case $a/s = 0.00$ nominally corresponds to the stator leading edge lying in the center of the IGV wake street, but the accuracy of positioning is at best 0.05. The IGV wake regions are again identified from the bands of higher turbulence level reaching values of over 2%. They are now more diffuse than at the rotor exit, and the minimum background turbulence level has risen to 1%. The minimum total disturbance level Tu_D is much higher at about 3%, indicating the effect of unsteadinesss from passing rotor wakes. The clocking effect is clearly evident from the movement of the higher turbulence bands and associated concentrations of low energy rotor wake fluid which appear as darker regions of low ensemble average velocity. The peak turbulence level outside the stator wakes, which occurs near these low velocity regions, reaches values of over 7% - a surprisingly high value for a compressor. There is a noticeably greater fluctuation in stator wake thickness for $a/s = 0.25$ and 0.50, which is most clearly evident on the suction side.

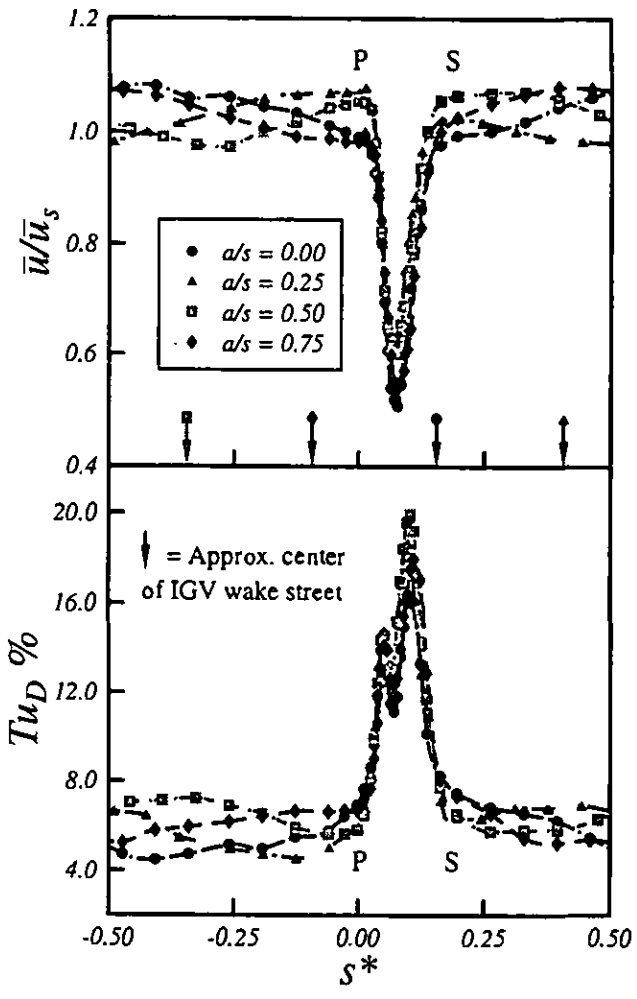

FIGURE 3: Influence of IGV clocking on circumferential variation of time mean velocity and total disturbance level. Hot-wire measurements 13.3% chord axially downstream of stator trailing edge at mid-passage. $\phi = 0.600$, $Re_{ref} = 120{,}000$. S = suction side; P = pressure side.

The circumferential variations of time-mean velocity and total disturbance level for different a/s values at the high loading case of $\phi = 0.600$ have been superimposed in Fig. 3 to indicate more clearly the effects of IGV clocking. Variations of up to 10% in $\overline{u}/\overline{u}_s$ and 3% in Tu_D outside the stator wake region can be seen to move in phase with the IGV wake street. The amplitude of these periodic circumferential variations in the mean flow is strongly loading dependent, and evidently associated with the strength of the rotor wakes. The variation in $\overline{u}/\overline{u}_s$ reduces to about 5% for $\phi = 0.675$ (see Fig. 4) and 2% for $\phi = 0.840$. The minimum values of Tu_D are again much higher than those of Tu, indicating a significant level of periodic fluctuation $\tilde{T}u$ in the free-stream region. Note that the local peak values of Tu_D outside the stator wakes correspond to circumferential positions where there is a lower time-mean velocity due to local accumulation of low energy fluid within the rotor wakes. A similar feature, with lower amplitude, is evident in Fig. 4.

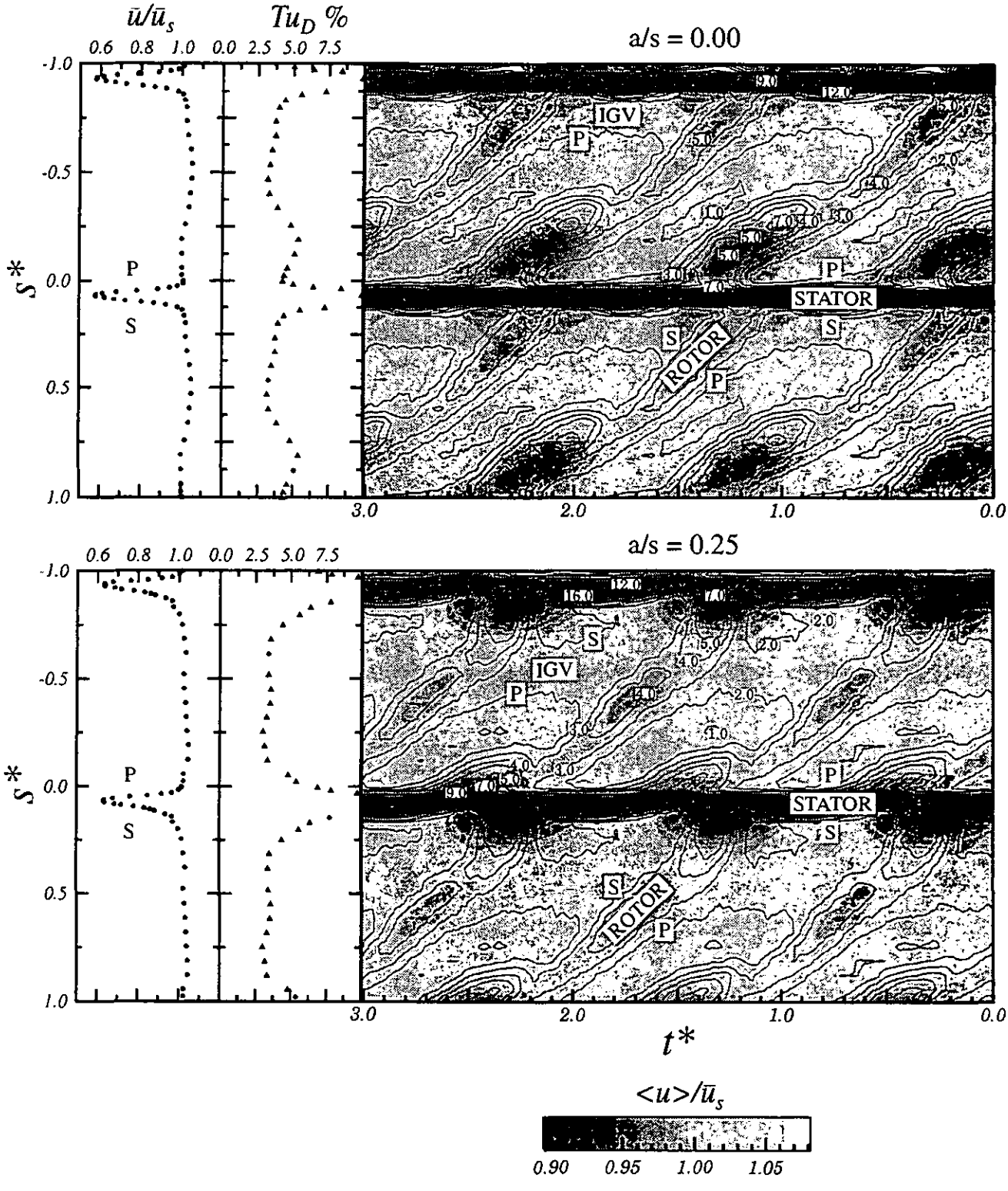

FIGURE 4: Influence of IGV clocking on unsteady flow field downstream of stator. Hot-wire measurements 13.3% chord axially downstream of stator trailing edge at mid-passage. a/s indicates circumferential position of stator blades relative to center of IGV wake street. Line contours indicate ensemble average turbulence level, $\langle Tu \rangle$ (%). ϕ = 0.675, Re_{ref} = 120,000. S = suction side; P = pressure side.

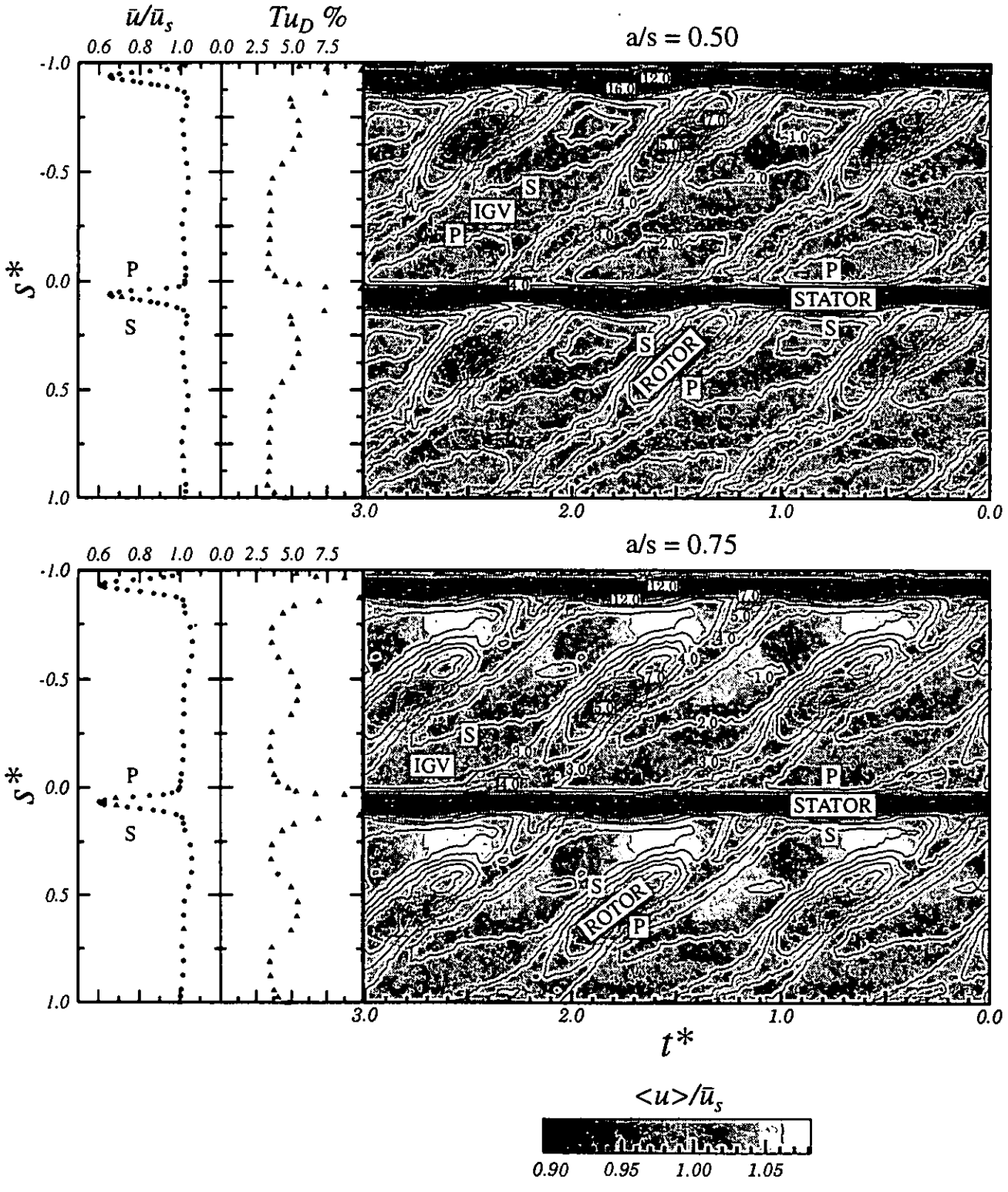

Evaluation of Stator Wake Properties

It is of interest to evaluate the stator wake properties to provide some quantitative indication of the influence of IGV clocking on stator losses. This is not a trivial problem, however, because of the non-uniform free-stream outside the stator wake region. Fig. 5 shows typical circumferential distributions of ensemble average velocity and turbulence obtained downstream of the stator at several different values of dimensionless time t^*. The free-stream flow is not uniform at any stage, and there is a differential in free-stream velocity across the stator wake which changes sign with the phase of the rotor wake passage. These variations may result from non-uniform energy addition, vortex shedding phenomena, redistribution of low energy fluid associated with intra-wake relative flows, or a combination of all three effects.

An algorithm for identifying the stator wake region was developed by examining changes in curvature of the ensemble average velocity profile. It was considered that a local peak in curvature would generally occur just inside the wake boundary. This provided an adequate means of identification in the majority of cases, but there were still some situations where no distinct peak in curvature occurred. Such ambiguities were resolved by further considering changes in slope of the turbulence distributions, thus making possible a completely automatic processing of the wake data. A typical example of an ensemble average velocity profile with the identified wake edge points is shown in Fig. 6.

Having decided on the wake boundaries, it is next necessary to prescribe an appropriate inviscid velocity distribution $U_{inv}(s^*)$ so that the wake properties can be evaluated. Two alternative models were considered:

(a) a constant value equal to the local velocity at the wake edge point; and
(b) a 3rd power polynomial of best fit to several points outside the wake edge.

The polynomial fit would be the more appropriate model if the free-stream region were a steady inviscid flow. However, that is not true in the present case where free-stream velocity variations may result from variable energy addition and loss redistribution phenomena.

For each of the above models, the hypothetical inviscid distribution was extrapolated to the circumferential position corresponding to the minimum velocity within the wake. A discontinuity in the inviscid distribution was allowed to occur at this location, and momentum thickness values for the pressure and suction side shear layers were calculated separately from

$$(\theta)/s = \int_0^1 \frac{\overline{u}/\overline{u}_s}{U_{inv}/\overline{u}_s}\left[1 - \frac{\overline{u}/\overline{u}_s}{U_{inv}/\overline{u}_s}\right]\cos\alpha ds^*\Big|_{t^*=const} \quad (7)$$

where α is the mean flow angle from axial. The separate thicknesses for the two shear layers were finally added to give the momentum thickness value for the whole wake.

It should be noted that purely inviscid flow modelling requires a velocity discontinuity within the wake region to represent the pressure differential which exists across a curved shear layer.

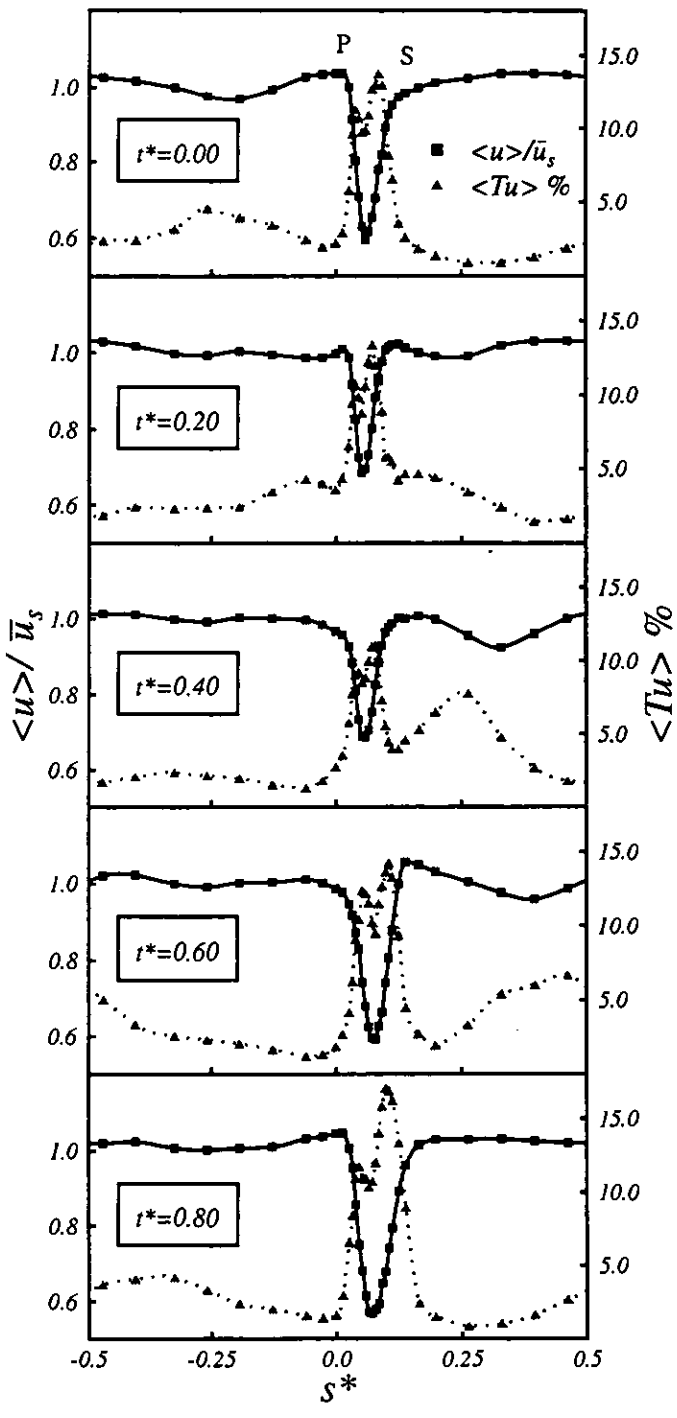

FIGURE 5: Typical variation in circumferential distributions of ensemble mean velocity and turbulence with phase of rotor wake passage. Hot-wire measurements 13.3% chord axially downstream of stator trailing edge at mid-passage. ϕ =0.675, Re_{ref} = 120,000. S = suction side; P = pressure side.

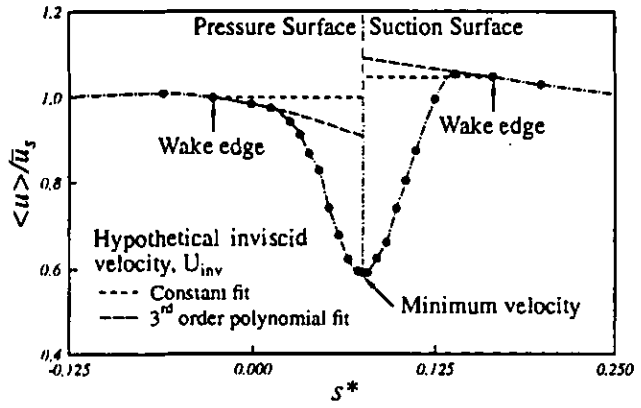

FIGURE 6: Alternative models for inviscid velocity distribution used for computing stator wake properties.

Influence of IGV Clocking on Stator Losses

A detailed discussion of compressor blade losses and their evaluation has been given by Cumpsty (1989). For steady two-dimensional cascade flow the wake momentum thickness at the normal outlet measuring station (around one chord length downstream of the blades) can be related to the total pressure loss coefficient for the cascade using the expression developed by Lieblein and Roudebush (1956).

It is assumed here that the values of wake momentum thickness evaluated by the above procedure from the measurements 13.3% chord axial distance downstream of the stator trailing edge will be reasonably representative of the stator blade viscous losses. A significant proportion of the wake mixing losses will have occurred by this stage, where the maximum observed value of wake velocity profile shape factor H was about 1.4. All of the momentum thickness data presented here has been evaluated using the 3rd power polynomial fit for the hypothetical inviscid flow model. Momentum thickness values obtained from the constant inviscid velocity model are about 10% greater on average, and this indicates the order of accuracy which can be expected in the absolute values of momentum thickness. There are no detectable differences in behavior between these momentum thickness values and the total pressure loss coefficient values calculated from Lieblein and Roudebush's (1956) analysis.

Both the time-mean and ensemble average values of wake momentum thickness are of interest. The time-mean value is relevant to blade row efficiency, whilst temporal variations in ensemble average values provide information on periodic fluctuations in shear layer thickness associated with wake-induced transition on the stator blade surfaces. Studies by Cumpsty et al. (1995), Halstead et al. (1995) and Solomon and Walker (1995b) all provide evidence of a greater susceptibility to turbulent separation of the thicker boundary layer regions within wake-induced turbulent strips. It is therefore conceivable that an increased level of unsteadiness in wake properties could indicate reduced stall margins.

Fig. 7 shows the influence of IGV clocking on the temporal variation of ensemble average stator wake momentum thickness for the medium loading case of $\phi = 0.675$. Values of $\langle\theta\rangle/s$ have been evaluated at intervals of $t^* = 0.03$ and smoothed with a 4th power best fit polynomial to 5 adjacent points on each side of the point under consideration. The variation of $\langle\theta\rangle/s$ with t^* is broadly sinusoidal, with phase differences of $\pm$ 0.1 in t^* according to the dimensionless IGV wake street location a/s.

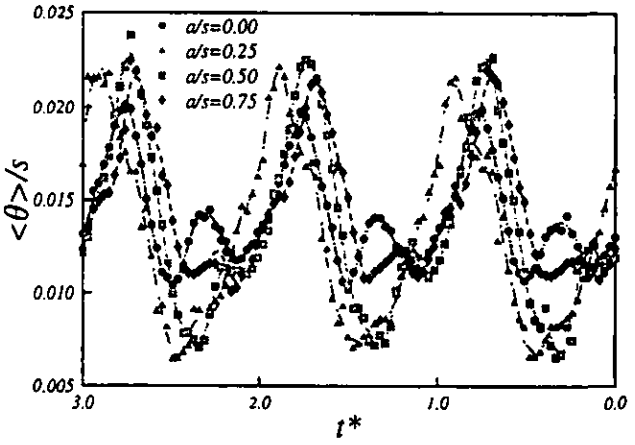

FIGURE 7: Influence of IGV clocking on temporal variation of ensemble average stator wake momentum thickness. Hot-wire measurements 13.3% chord axially downstream of stator trailing edge at mid-passage. $\phi = 0.675$, $Re_{ref} = 120{,}000$.

The periodic variation in $\langle\theta\rangle/s$ noted previously from Fig. 4 is more clearly evident in Fig. 7. Its amplitude is greatest for a/s = 0.25 and 0.50. when the IGV wake street passes through the center of the blade passage and the stator blades are subjected to higher levels of periodic unsteadiness from the passing rotor wake disturbances. Here the maximum value of $\langle\theta\rangle/s$ is nearly 4 times the minimum.

The lowest level of unsteadiness in the stator wake thickness occurs for $a/s = 0.00$, when the IGV wake street is incident on the stator blade leading edge. Here the ratio of maximum to minimum $\langle\theta\rangle/s$ has fallen to around 2. This reduction is mostly due to an increase in the minimum value of $\langle\theta\rangle/s$, but the maximum value is nevertheless about 10% lower than that for $a/s = 0.50$.

The results for all three loading cases have been summarised in Table 1. The time-mean values of dimensionless wake momentum thickness $\overline{\theta}/s$ have been evaluated from an average of the ensemble means over three rotor blade passing periods. The degree of unsteadiness in the stator wake is indicated by the standard deviation in values of $\langle\theta\rangle/s$ over the same interval.

There is a consistent trend in the data for significantly higher values of wake unsteadiness, S.D. ($\langle\theta\rangle/s$), at $a/s = 0.25$ and 0.50. The minimum value of S.D. ($\langle\theta\rangle/s$) always occurs for $a/s = 0.00$. when the stator blades are immersed in the IGV wake street, although the unsteadiness for $a/s = 0.75$ is closely comparable.

It is difficult to draw firm conclusions on the values of time-mean wake thickness $\overline{\theta}/s$, as these show no clear trend. The fluctuation in $\overline{\theta}/s$ with a/s is similar in magnitude to the uncertainty in evaluating $\overline{\theta}/s$ from different models for $U_{inv}(s^*)$ for all three loading cases. Values of $\overline{\theta}/s$ for the minimum unsteadiness configuration of $a/s = 0.00$ are slightly less than the average for all a/s values with polynomial $U_{inv}(s^*)$ model; but with the constant $U_{inv}(s^*)$ model they tend to be about the average of $\overline{\theta}/s$ over all a/s val-

TABLE 1: Influence of IGV clocking and flow coefficient on time-mean stator wake thickness and stator wake unsteadiness

ϕ	a/s	$\overline{\theta}/s$	S.D. $(\langle\theta\rangle/s)$ (%)
0.600	0.00	0.0175	32
	0.25	0.0187	46
	0.50	0.0185	49
	0.75	0.0190	32
0.675	0.00	0.0153	29
	0.25	0.0143	51
	0.50	0.0146	51
	0.75	0.0157	37
0.840	0.00	0.0111	14
	0.25	0.0121	35
	0.50	0.0113	33
	0.75	0.0123	14

ues. In summary, the evidence favors a slight reduction in loss for the minimum unsteadiness configuration. At least, there is no suggestion of a serious performance decrement in this case. There is certainly no evidence here which would negate the conclusions of Eulitz et al.'s (1996) numerical study of the influence of IGV clocking on axial turbine performance.

It is stressed that only a single blade element has been considered here. The blade elements at different radii will lie at different values of a/s due to skewing of the IGV wake street associated with the radial flow distribution in the compressor. The integrated effect on performance for the whole stator blade will therefore be less than that for an isolated element. No significant variation in flow coefficient could be detected with IGV clocking at constant throttle.

The fluctuations in ensemble average stator wake thickness $\langle\theta\rangle/s$ for the minimum and maximum unsteadiness configurations of a/s = 0.00 and a/s = 0.50 are shown in Fig. 8 for all three loading cases. The suction and pressure side contributions to the total wake thickness are shown separately. Whilst there may have been some decay in wake asymmetry in the 13.3% chord axial distance downstream of the trailing edge, these curves should give a useful indication of the loss fluctuations on the individual blade surfaces. Additional data obtained at 1.5% chord axial distance downstream of the stator for a more limited range of conditions are presented by Solomon (1996).

For a/s = 0.00 and ϕ = 0.840 the pressure and suction side fluctuations are almost identical, with the exception of an asymmetrical feature around t^* = 0, 1, 2 which is suggestive of potential flow interaction effects as the rotor wakes pass over the stator leading edge. This asymmetry develops with increases in loading to ϕ = 0.675 and 0.600. There is a simultaneous increase in the relative thickness of the suction side layer, and a phase lead develops in the suction side perturbation due to the effects of blade circulation. The oscillations in individual shear layer thicknesses are clearly indicative of periodic wake-induced transition in the blade boundary layers. They closely resemble the measured boundary layer thickness fluctuations in the unsteady compressor cascade tests of Cumpsty et al. (1995) and the multistage compressor tests of Halstead et al. (1995). The fluctuations in total wake momentum thickness have developed harmonic content due to the combination of these two out-of-phase components.

The general behavior is quite similar for the maximum stator wake unsteadiness configuration of a/s = 0.50. However, there is much greater periodicity and the ratio of maximum to minimum momentum thickness is significantly greater for both shear layer components in all three loading cases. It is particularly interesting to note that the peak values of $\langle\theta\rangle/s$ for a/s = 0.50 are typically 10% higher than the corresponding values for a/s = 0.00. This suggests that the stator blades should be more resistant to intermittent separation and stall in the latter case, when the stator blades are immersed in the IGV wake street.

Physical Model for Stator Wake Unsteadiness

The amplitude of the stator wake unsteadiness can be explained in terms of transition phenomena on the blade surface. The peak momentum thickness corresponds to the boundary layer thickening caused by wake-induced transition initiated by the rotor wakes. This is slightly lower for the case a/s = 0.0, where the IGV wake street is incident on the stator blade and the amplitude of rotor wake disturbances is somewhat lower because of IGV wake-rotor wake interactions.

The minimum momentum thickness in the stator wake corresponds to later transition within the stator blade boundary layers in the region between the rotor wakes. This is controlled by other modes - principally bypass transition and separated flow transition. Bypass transition depends on the level of free-stream turbulence, which varies from the backgound inlet turbulence level of about 0.5% to around 3% within the IGV wake street.

Whilst the peak turbulence in the IGV wakes varies little with loading, the average turbulence over the region between rotor wakes steadily increases with loading. This follows from the increased dispersion of IGV wakes associated with higher rotor circulation. It is interesting to note that the ratio of maximum to minimum stator wake thickness also decreases steadily as loading is increased. This is suggestive of stronger bypass transition between the rotor wakes causing a more uniform stator wake. Similar effects could be expected to occur with changes in rotor-stator axial gaps.

CONCLUSIONS

The dispersion of inlet guide vane wakes by the rotor, and subsequent interactions between the IGV and rotor blade wakes, produced regular circumferential variations in both the time-mean and unsteady flow downstream of the rotor in the test compressor. The influence of these variations on stator losses was examined through ensemble average measurements of the stator wake properties.

Separate evaluation of the suction and pressure side momentum thickness components for the stator wake proved very useful. The individual components showed a lower harmonic content than the composite wake thickness, which was influenced by phase lags between periodic wake-induced phenomena on the stator blade suction and pressure surfaces.

Significantly lower amplitudes of periodic fluctuations in the stator wake were observed when the stator blades were immersed in the avenue of dispersed IGV wake segments. The peak values of shear layer thickness were always lower in this configuration.

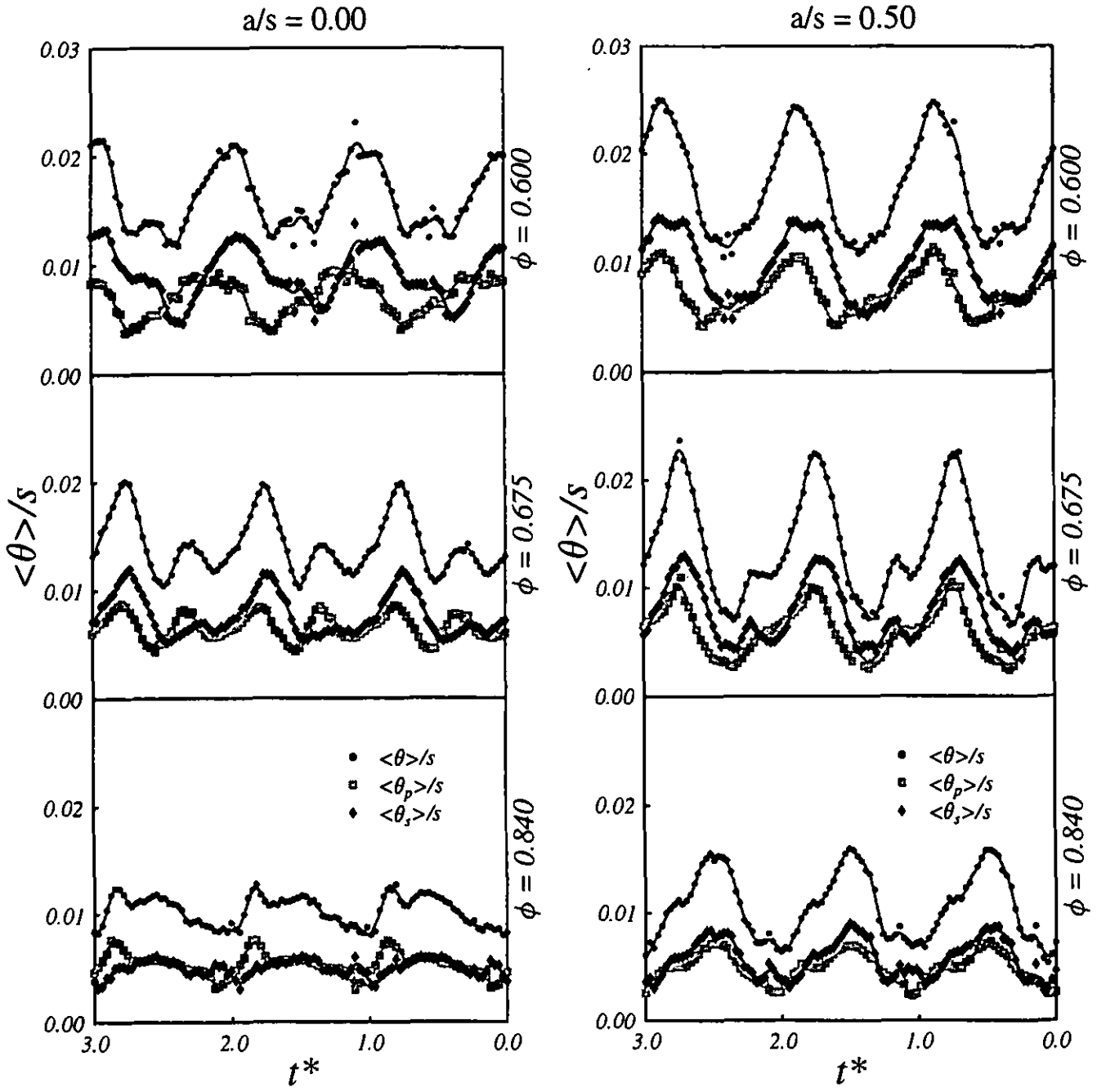

FIGURE 8: Temporal variation of stator wake momentum thickness 13.3% chord axially downstream of stator trailing edge at mid-passage, showing division into pressure and suction side components and influence of IGV clocking. Re_{ref} = 120,000

It is considered that this should make the stator blades less susceptible to intermittent separation and stall. No firm conclusions could be drawn about the time-mean stator loss values in this case, as the observed variation in losses was comparable in magnitude with the uncertainty in the data. However, there was certainly no serious performance deterioration.

The unsteady variations of flow behavior on blade surfaces and in the wakes are strong and should be taken into account when determining blade clocking effects and rotor-stator axial gaps for axial turbomachines.

ACKNOWLEDGMENTS

The authors wish to acknowledge the support of the Australian Research Council and Rolls-Royce plc.

They are also indebted to reviewers for their thorough consideration of the manuscript and helpful comments.

Mr Jason Roberts provided valuable advice on typesetting of the manuscript.

REFERENCES

Adamczyk, J. J., 1996, "Wake Mixing in Axial Flow Compressors," ASME Paper 96-GT-29, Birmingham.

Cumpsty, N. A., 1989, *Compressor Aerodynamics*, First edn., Longman Scientific & Technical.

Cumpsty, N. A., Dong, Y., and Li, Y. S., 1995, "Compressor Blade Boundary Layers in the Presence of Wakes," ASME Paper 95-GT-443, Houston.

Deregel, P., and Tan, C. S., 1996, "Impact of Rotor Wakes on Steady-State Axial Compressor Performance," ASME Paper 96-GT-253, Birmingham.

Eulitz, F., Engel, K., and Gebing, H., 1996, "Numerical Investigation of Clocking Effects in a Multistage Turbine," ASME Paper 96-GT-26, Birmingham.

Evans, R. L., 1975, "Turbulence and Unsteadiness Measurements Downstream of a Moving Blade Row," *ASME Journal of Engineering for Power*, pp. 131–139.

Gostelow, J. P., Walker, G. J., Solomon, W. J., Hong, G., and Melwani, N., 1996, "Investigation of the Calmed Region Behind a Turbulent Spot," ASME Paper 96-GT-489, Birmingham.

Halstead, D. E., Wisler, D. C., Okiishi, T. H., Walker, G. J., Hodson, H. P., and Shin, H-W, 1995, "Boundary Layer Development in Axial Compressors and Turbines: Parts 1–4," ASME Papers 95-GT-461–464.

Hourmouziadis, J., 1989, "Aerodynamic Design of Low Pressure Turbines," pp. 8–1–8–40, Fottner, L. (ed), *AGARD Lecture Series No. 167, Blading Design for Axial Turbomachines*, AGARD.

Howell, A. R., 1945, "Fluid Dynamics of Axial Compressors," *Proc. Inst. Mech. Eng. E*, Vol. 153, pp. 441–452.

Kerrebrock, J. L., and Mikolajczak, A. A., 1970, "Intra-Stator Transport of Rotor Wakes and Its Effect on Compressor Performance," *ASME Journal of Engineering for Power*, Vol. 92, pp. 359–368.

Lieblein, S., and Roudebush, W., 1956, "Theoretical Loss Relations for Low-Speed Two-Dimensional Cascade Flow," NACA TN 3662.

Lockhart, R. C., and Walker, G. J., 1974, "The Influence of Viscous Interactions on the Flow Downstream of an Axial Compressor Stage," Paper presented at the 2nd International Symposium on Air Breathing Engines.

Mayle, R. E., 1991, "The Role of Laminar-Turbulent Transition in Gas Turbine Engines," *ASME Journal of Turbomachinery*, Vol. 113, pp. 509–537, The 1991 IGTI Scholar Lecture.

Mayle, R. E., 1992, "Unsteady Multimode Transition in Gas Turbine Engines," AGARD PEP 80.

Oliver, A. R., 1961, "Comparison Between Sand Cast and Machined Blades in the Vortex Wind Tunnel," Report ME 103, Aeronautical Research Laboratories, Melbourne, Australia.

Schulte, V., and Hodson, H. P., 1996, "Unsteady Wake-Induced Boundary Layer Transition in High Lift LP Turbines," ASME Paper 96-GT-486, Birmingham.

Smith Jr., L. H., 1966, "Wake Dispersion in Turbomachines," *ASME Journal of Basic Engineering*, Vol. 88, pp. 688–690.

Solomon, W. J., 1996, "Unsteady Boundary Layer Transition on Axial Compressor Blades," Ph.D. Thesis, University of Tasmania.

Solomon, W. J., and Walker, G. J., 1995a, "Incidence Effects on Wake-Induced Transition on an Axial Compressor Blade," *Proc. 12th Int. Symp. on Air Breathing Engines*, Vol. 2, pp. 954–964, ISABE 95-7088, Melbourne.

Solomon, W. J., and Walker, G. J., 1995b, "Observations of Wake-Induced Transition on an Axial Compressor Blade," ASME Paper 95-GT-381, Houston.

Suryavamshi, N., Lakshminarayana, B., and Prato, J., 1996, "Aspirating Probe Measurements of the Unsteady Total Temperature Field Downstream of an Embedded Stator in a Multistage Axial Flow Compressor," ASME Paper 96-GT-543, Birmingham.

Walker, G. J., 1972, "An Investigation of the Boundary Layer Behaviour on the Blading of a Single-Stage Axial-Flow Compressor," Ph.D. Thesis, University of Tasmania.

Walker, G. J., 1974, "The Unsteady Nature of Boundary Layer Transition on an Axial Compressor Blade," ASME Paper 74-GT-135.

Walker, G. J., 1975, "Observations of Separated Laminar Flow on Axial Compressor Blading," ASME Paper 75-GT-63, Houston.

Walker, G. J., 1993, "The Role of Laminar-Turbulent Transition in Gas Turbine Engines — A Discussion," *ASME Journal of Turbomachinery*, Vol. 117, pp. 207–217.

Zierke, W. C., and Okiishi, T. H., 1982, "Measurement and Analysis of Total-Pressure Unsteadiness Data from an Axial Compressor Stage," *ASME Journal of Engineering for Power*, Vol. 104, pp. 479–488.